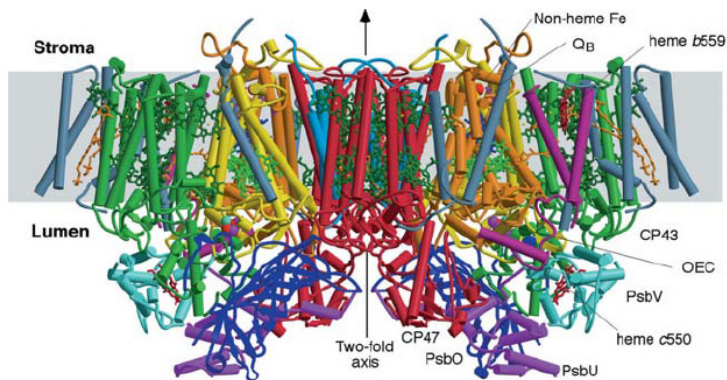




BioSolar Cells

Global and target analysis of
energy transfer and quenching
in the thylakoid membrane

Ivo H.M. van Stokkum
Computational Biophysics



A 3D ribbon diagram of a large protein complex, likely a viral capsid, showing multiple subunits in various colors (green, yellow, blue, purple, pink) arranged in a symmetrical, spherical structure.

Q: how to study the function of PS I of Cyanobacteria ?

A: by measuring the time resolved emission spectrum with high time resolution using 400 nm (Soret) excitation with low power to avoid annihilation

And then try to model it ...

Lorentz
center

Modeling Natural and Artificial Photosynthesis

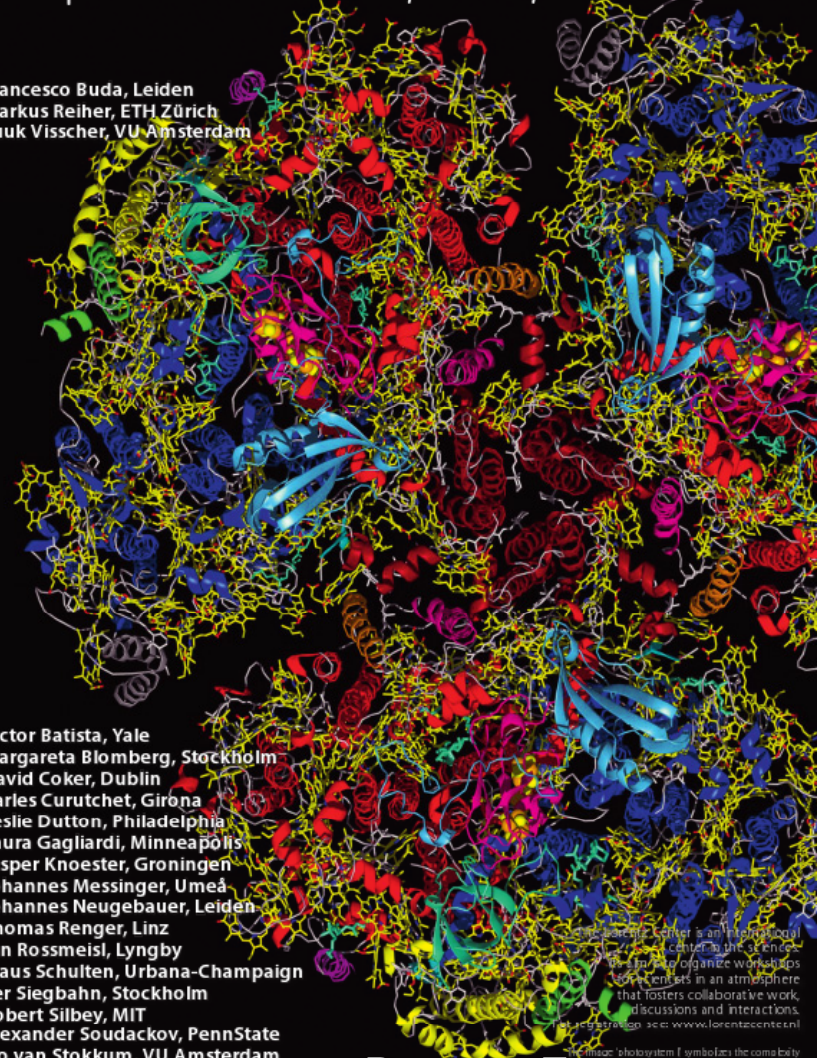
Workshop: 7 - 11 March 2011, Leiden, the Netherlands

Scientific Organizers

- Francesco Buda, Leiden
- Markus Reiher, ETH Zürich
- Luuk Visscher, VU Amsterdam

Invited Speakers

- Victor Batista, Yale
- Margareta Blomberg, Stockholm
- David Coker, Dublin
- Carles Curutchet, Girona
- Leslie Dutton, Philadelphia
- Laura Gagliardi, Minneapolis
- Jasper Knoester, Groningen
- Johannes Messinger, Umeå
- Johannes Neugebauer, Leiden
- Thomas Renger, Linz
- Jan Rossmeisl, Lyngby
- Klaus Schulten, Urbana-Champaign
- Per Siegbahn, Stockholm
- Robert Silbey, MIT
- Alexander Soudackov, PennState
- Ivo van Stokkum, VU Amsterdam
- Joost VandeVondele, UZH Zürich



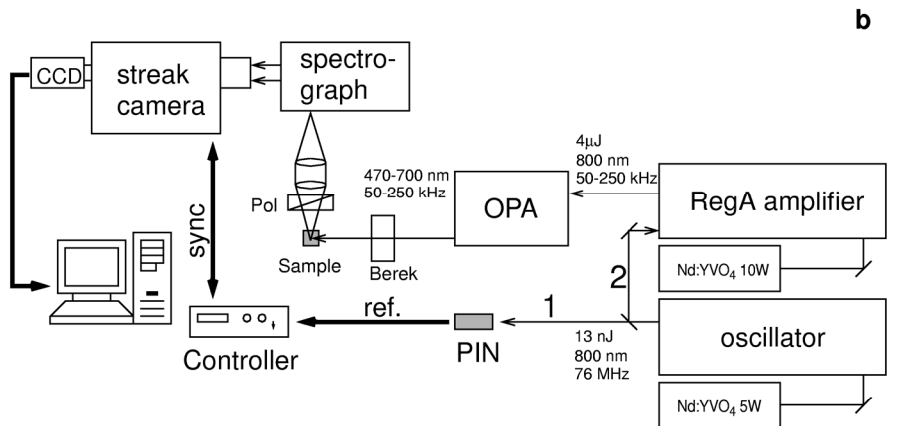
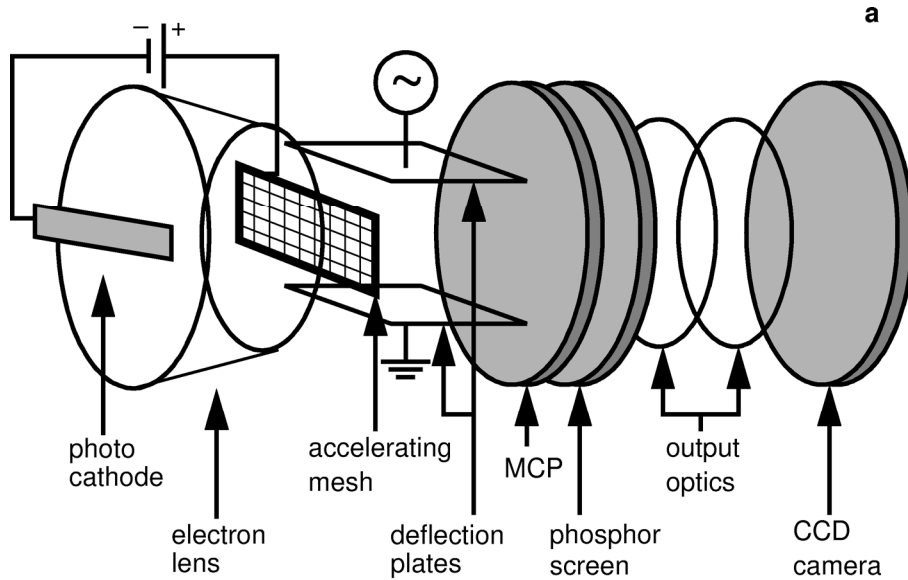
Petra Fromme



Lorentz
center

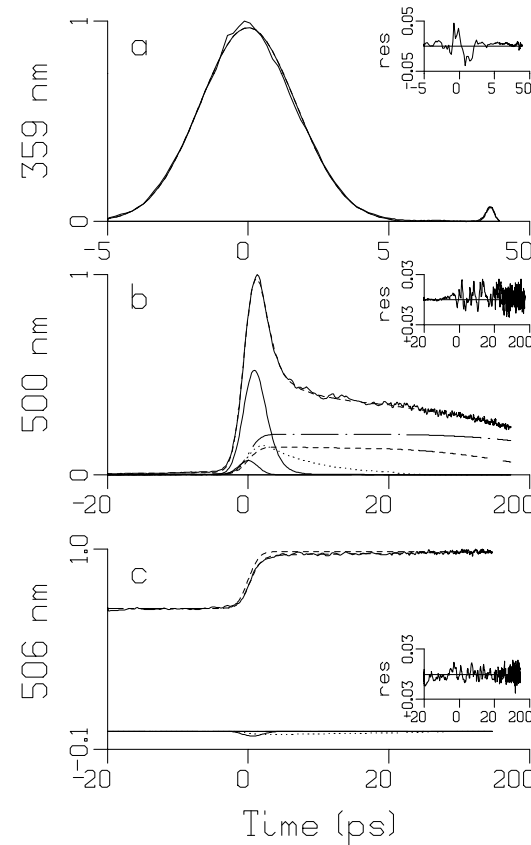
www.lorentzcenter.nl

Time resolved emission



Synchroscan streak scope

Instrument Response Function
at best ~ 4 ps FWHM

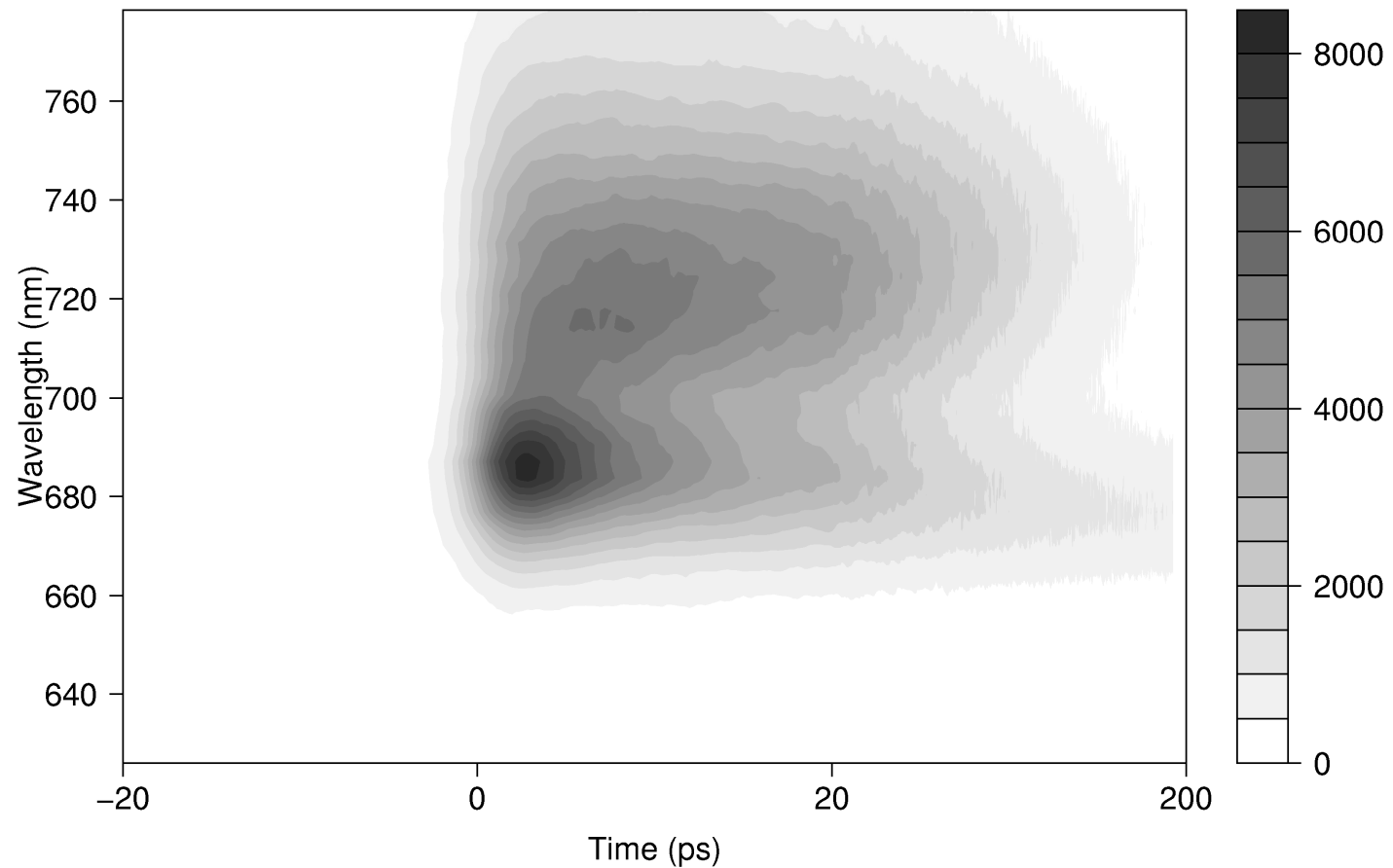


IRF

1.2 ps
decay

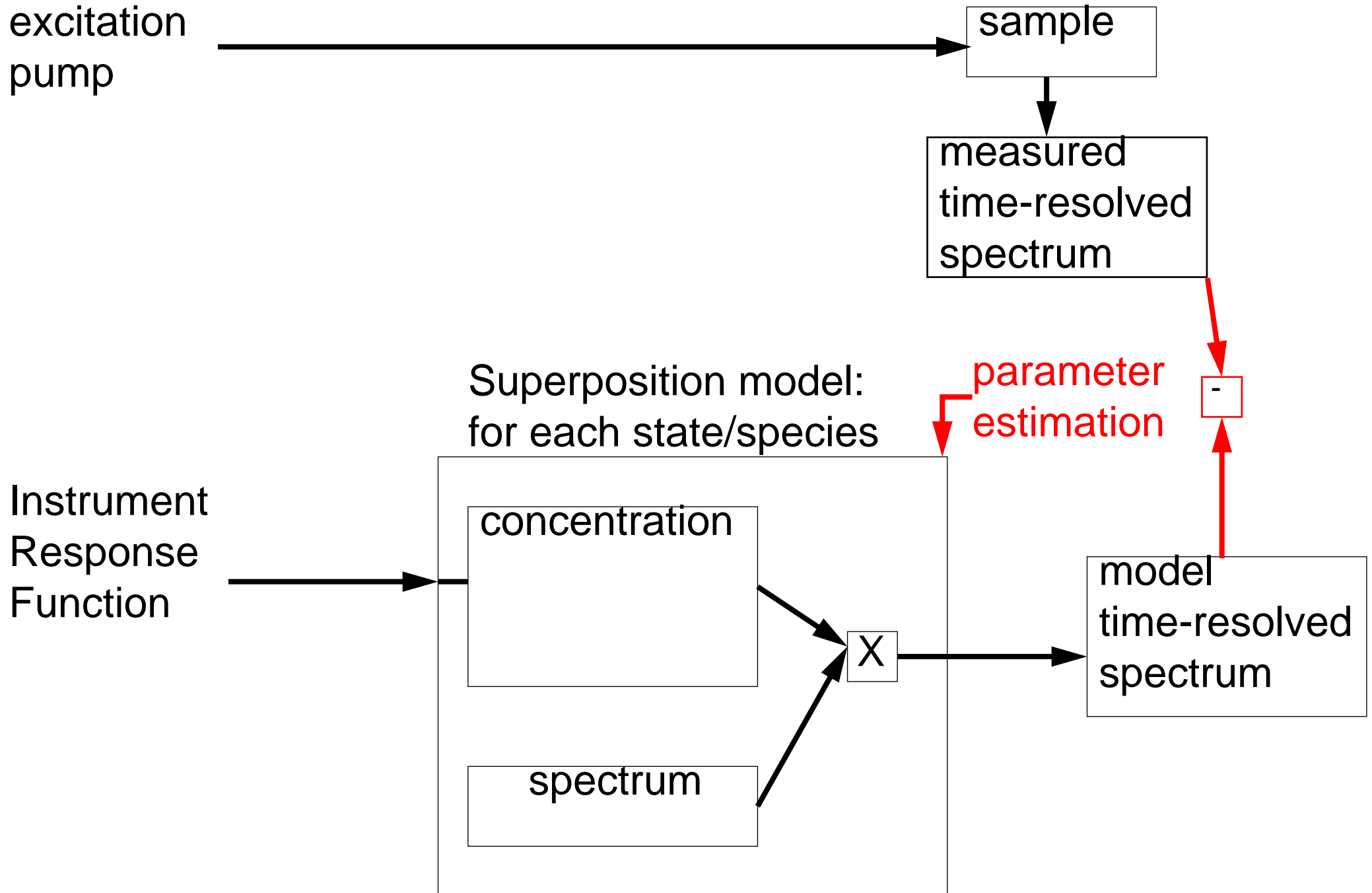
17 ns
decay

Measured PS I core emission $\Psi(\lambda, t)$



Q: How to analyse and model phenomenologically?

Modelling and parameter estimation scheme



Global and target analysis

Multiple experiments (detection wavelength, polarization angle, excitation wavelength, ...) at possibly multiple physiological conditions (temperature, pH, pD, open/closed RC, (un)quenched, ...) are simultaneously analysed. Their information is integrated, and the parameters θ are estimated more precisely. When the residuals are satisfactory, the **target** model that is tested can be considered an adequate description of the data.

After fitting the data globally with a sufficient number of exponential decays (lifetimes) different compartmental schemes (target models) are tested.

Adequacy of a model can be judged from the plausibility of the estimated parameters, in particular the spectral shapes, and the microscopic rate constants. In case of equilibria also the free energy differences can be

computed $\Delta G = k_B T \ln \left(\frac{k_{\text{forward}}}{k_{\text{backward}}} \right)$.

Superposition model for the observations

$$\Psi_{qt_i\lambda_j} = \sum_{l=1}^{n_{\text{comp},\lambda_j}} c_{q\lambda_j t_i l}(\Theta) \varepsilon_{\lambda_j l} = C_{q\lambda_j}(\Theta) \varepsilon_{\lambda_j} + \xi_{qt_i\lambda_j}$$

experiment q , $q = 1, \dots, Q$,

time point t_i , $i = 1, \dots, n_{t,q}$

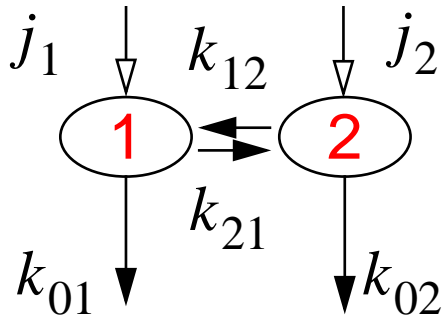
$n_{\text{comp},\lambda_j}$ number of components that contribute at

wavelength λ_j , $j = 1, \dots, n_{\lambda,q}$

additive normally distributed noise $\xi_{qt_i\lambda_j}$

nonlinear least squares model with intrinsically nonlinear parameters Θ and conditionally linear parameters $\varepsilon_{\lambda_j l}$, ($l = 1, \dots, n_{\text{comp},\lambda_j}$), ($j = 1, \dots, n_{\lambda, \text{tot}}$)

Compartmental models

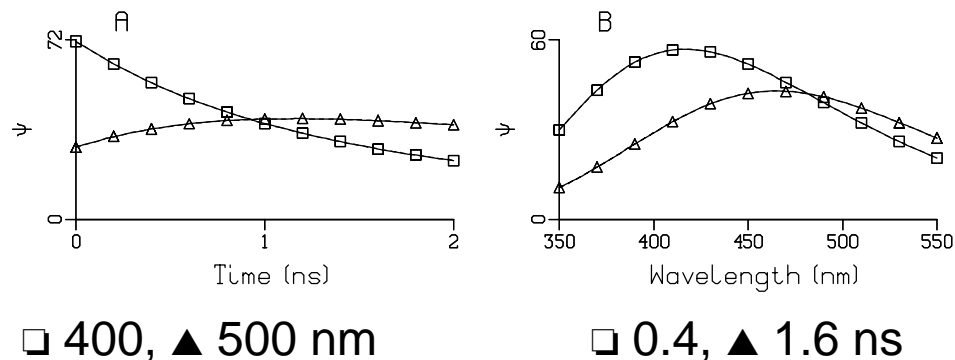


$$\frac{d}{dt} \begin{bmatrix} c_1(t) \\ c_2(t) \end{bmatrix} = \begin{bmatrix} -k_{01} - k_{21} & k_{12} \\ k_{21} & -k_{02} - k_{12} \end{bmatrix} \begin{bmatrix} c_1(t) \\ c_2(t) \end{bmatrix} + \begin{bmatrix} j_1 \\ j_2 \end{bmatrix} i(t)$$

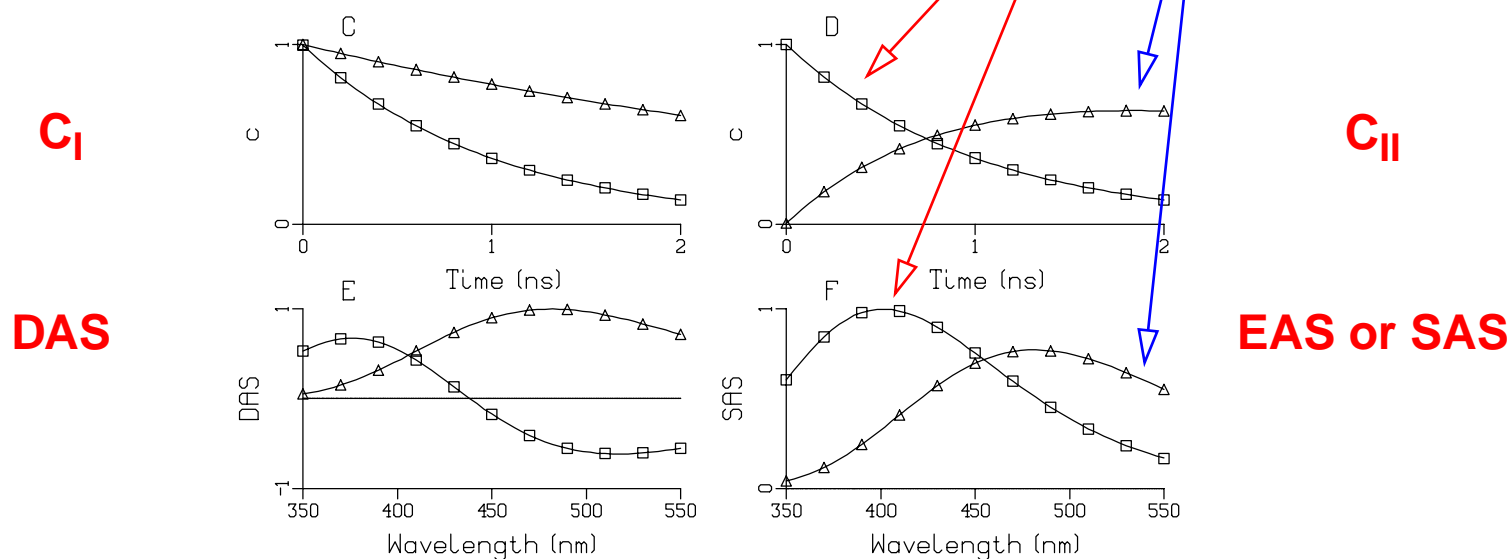
$$\frac{dc}{dt} = Kc + j(t) \quad c = \exp(Kt) \oplus j(t)$$

Solution: linear combination of exponential decays convolved with IRF $i(t)$

	K	j	c	$\Psi = CE^T$	spectral relation
parallel, decay associated	$\begin{bmatrix} -k_1 & 0 \\ 0 & -k_2 \end{bmatrix}$	$\begin{bmatrix} 1 \\ 1 \end{bmatrix}$	$\begin{bmatrix} \exp(-k_1 t) \\ \exp(-k_2 t) \end{bmatrix} \equiv C_I^T$	$C_I DAS^T$	
sequential, evolution associated, unbranched unidirectional	$\begin{bmatrix} -k_1 & 0 \\ k_1 & -k_2 \end{bmatrix}$	$\begin{bmatrix} 1 \\ 0 \end{bmatrix}$	$C_{II} = C_I R_{II}$	$C_{II} EAS^T$	$EAS R_{II}^T = DAS$
general, species associated			$C_{III} = C_I A_{III}$	$C_{III} SAS^T$	$SAS A_{III}^T = DAS$

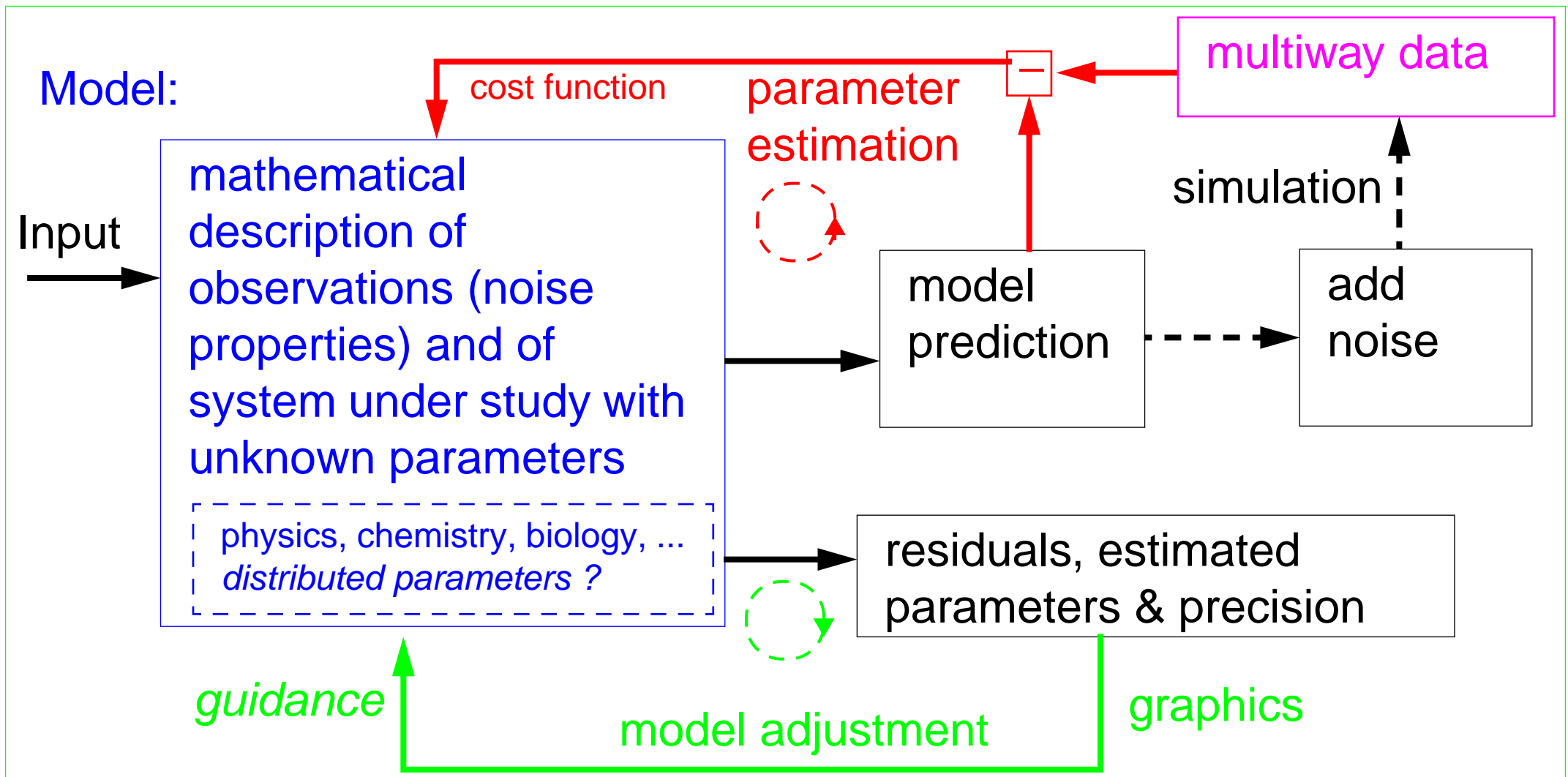


Simulated data: sequential scheme $1 \rightarrow 2$, $\Psi = C_{II}EAS^T$



Analysis with wrong, parallel, kinetic scheme results in unrealistic DAS, which indicate rise of long lived component, and suggest $1 \rightarrow 2$

A Problem Solving Environment for interactive modelling of multiway data



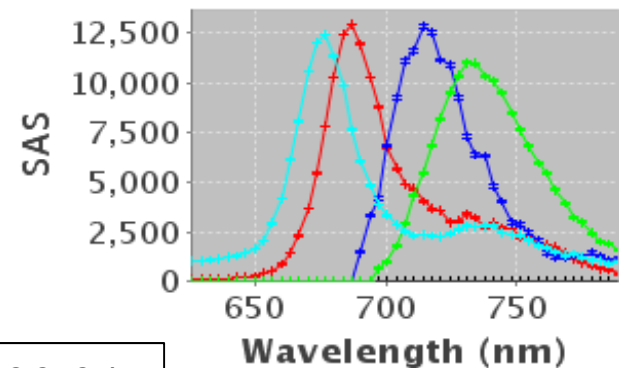
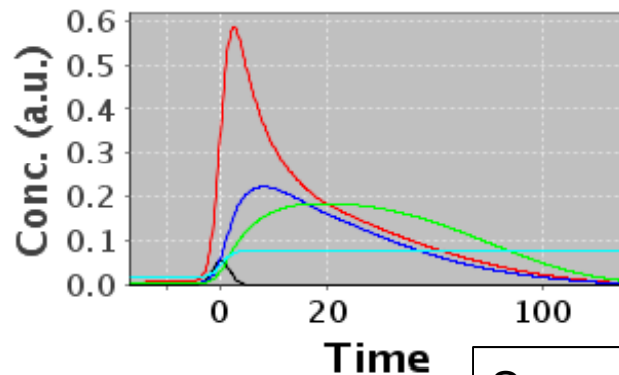
Glutaran

A tool for interactive global and target analysis of time-resolved spectroscopy and microscopy data



Joris Snellenburg, Sergey Laptenok, Katharine Mullen

- Open source, platform independent, developed on Java
- Uses the R-package TIMP as a computational back-end
- Interactive data-exploration and inspection of results
- Can be downloaded from glutaran.org



Supported by NWO CS grant 635.000.014

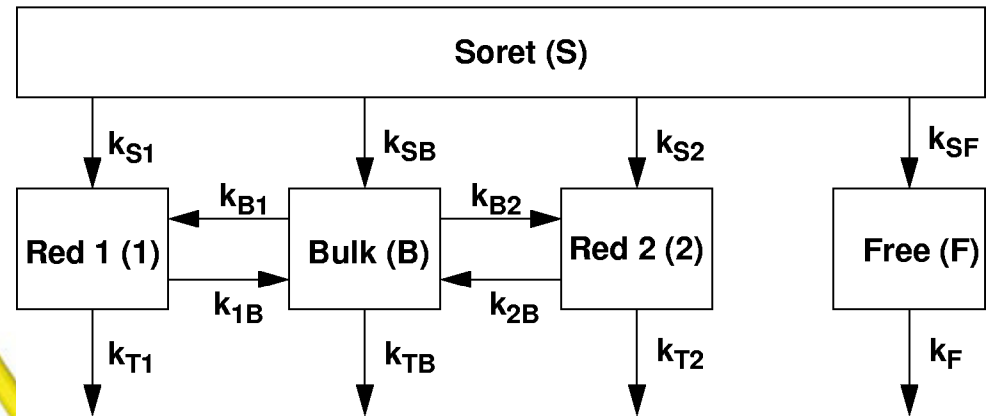
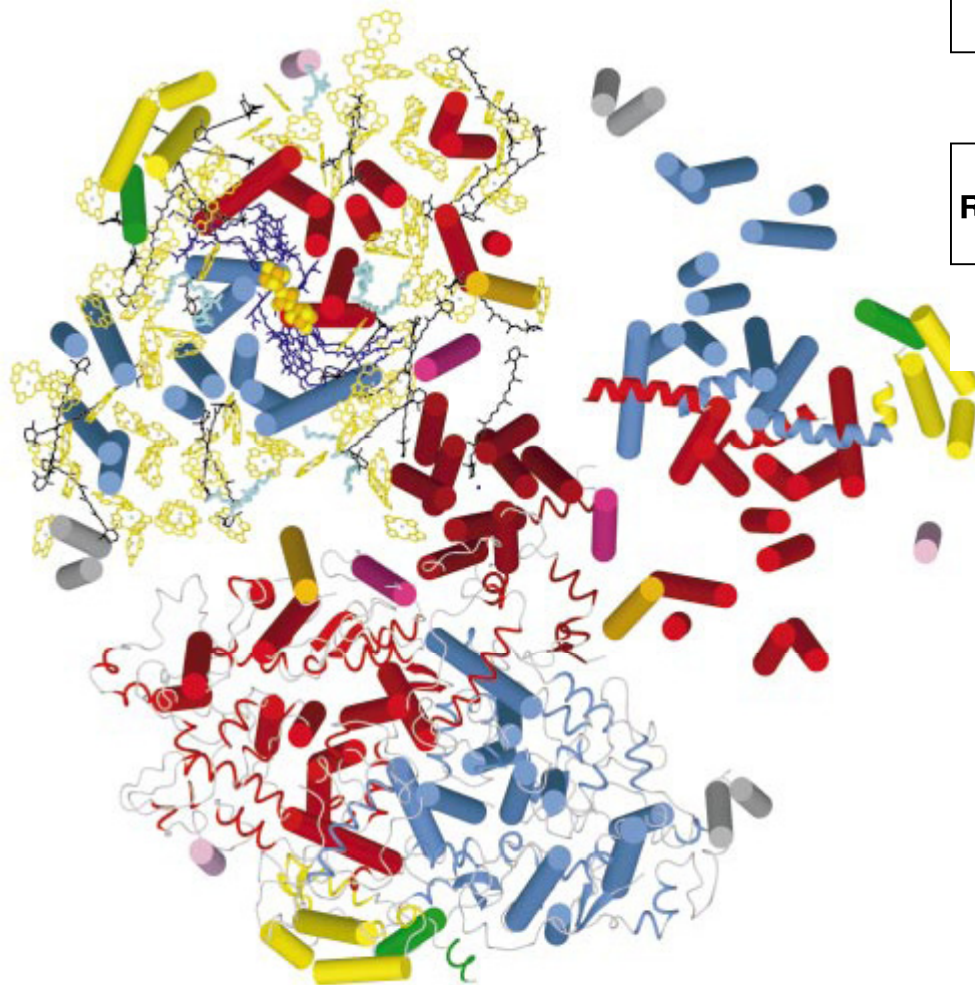


Netherlands Organisation for Scientific Research

vrije Universiteit amsterdam



Case study: cyanobacterial PS I core with two pools of red chlorophylls



Compartmental model with four types of Chls
Bulk, Red 1 and 2, and a small fraction Free

Photochemical quenching with
trapping rate $k_T \approx 1/(18 \text{ ps})$

Gobets, B., van Stokkum, I.H.M., Rogner, M., Kruip, J., Schlodder, E., Karapetyan, N.V., Dekker, J.P., van Grondelle, R. 2001b. Time-resolved fluorescence emission measurements of photosystem I particles of various cyanobacteria: A unified compartmental model. *Biophysical Journal* 81, 407-424.

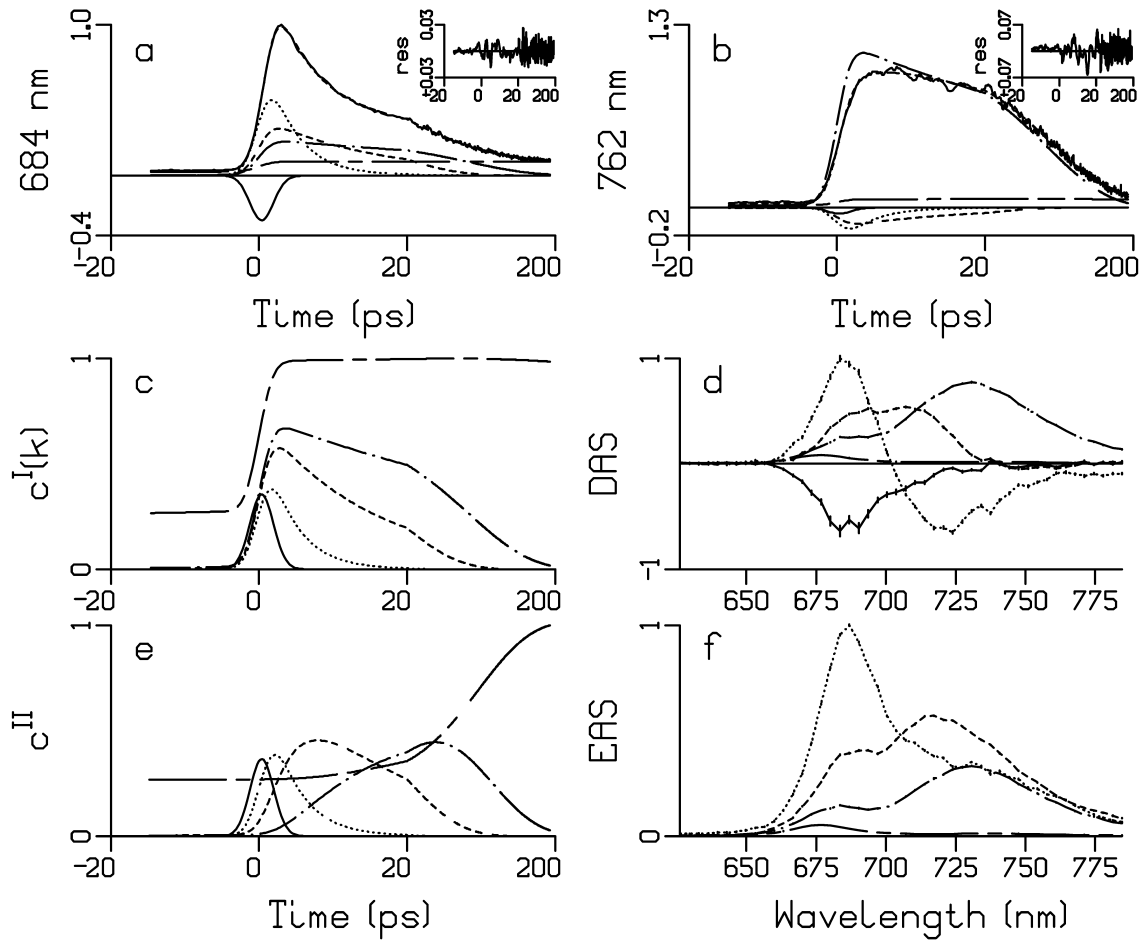


Fig. 4. Results from global analysis of PS I data depicted in Fig. 1. Note that in a–c and e the time axis is linear from –20 to +20 ps relative to the maximum of the IRF, and logarithmic thereafter. Insets in a, b show residuals. (a) Fit of bulk Chl *a* emission trace showing multiexponential decay. Contributions of the five exponential decays with different lifetimes (shown in c) are indicated by line type. (b) Fit of red Chl *a* emission trace showing multiexponential rise and decay. (c) Exponential decays $c^I(k)$. Estimated lifetimes: 0.4 ps (solid), 3.9 ps (dotted), 15 ps (dashed), 50 ps (dot dashed), and 4.9 ns (chain dashed). (d) Decay Associated Spectra (DAS), note that the first DAS which represents overall rise has been multiplied by 0.2. Vertical bars indicate estimated standard errors. (e) Evolutionary concentration profiles c^II (assuming a sequential kinetic scheme with increasing lifetimes). (f) Evolution Associated Spectra (EAS). Note that the first EAS is zero, since excitation was in the Soret band.

where each concentration is a linear combination of the exponential decays,

$$c_l^{II} = \sum_{j=1}^l b_{jl} c^I(k_j) \quad (13)$$

and the amplitudes b_{jl} are given by $b_{11} = 1$ and for $j \leq l$:

$$b_{jl} = \frac{\prod_{m=1}^{l-1} k_m}{\prod_{n=1, n \neq j}^l (k_n - k_j)} \quad (14)$$

Examples of c_l^{II} are depicted in Fig. 4e, whereas the EAS estimated from the PS I trimer data are shown in Fig. 4f. With increasing lifetimes, and thus decreasing rates k_j , the first EAS (equal to the sum of DAS) corresponds to the spectrum at time zero with an ideal

infinitely small IRF, $i(t) = \Delta(t)$. In Fig. 4f, this first EAS is zero in the Q_y region. The second EAS (dotted), which is formed in 0.4 ps and decays in 3.9 ps, represents the sum of the spectra of all excitations that have arrived from the Soret region, and is dominated by bulk Chl *a*. The third EAS, which is formed in 3.9 ps and decays in 15 ps, is already dominated by red Chl *a* emission, which is even more the case with the fourth EAS (dot dashed, formed in 15 ps, decays in 50 ps). The final EAS (chain dashed, formed in 50 ps) is proportional to the final DAS, and represents the spectrum of the longest living component (4.9 ns). Clearly, these EAS do not represent pure species, except for the final EAS, and they are interpreted as a weighted sum (with only positive contributions) of true species spectra.

(3) When neither of these two simple models is applicable, a full kinetic scheme may be appropriate. The problem with such a scheme is that, while the kinetics are described by microscopic rate constants, the data only allows for the estimation of decay rates (or lifetimes). Thus additional information is required to estimate the microscopic rates, which can be spec-

tral constraints (zero contribution of SAS at certain wavelengths) or spectral relations. This is explained in detail in van Stokkum et al. (2004).

Now the model reads:

$$\psi(t, \lambda) = \sum_{l=1}^{n_{comp}} c_l^{III} SAS_l(\lambda) \quad (15)$$

where the concentrations c_l^{III} are again linear combinations of the exponential decays, with coefficients that depend upon the microscopic rate constants that describe the transitions between all the compartments. Figure 5a depicts the kinetic scheme that was applied to the trimeric PS I data of Fig. 1. The concentrations of all compartments are collated in a vector $c(t) = [c_1(t) \ c_2(t) \ \dots \ c_{n_{comp}}(t)]^T = [S(t) \ B(t) \ R_1(t) \ R_2(t) \ F(t)]^T$, which obeys the differential equation:

$$\frac{d}{dt} c(t) = Kc(t) + j(t) \quad (16)$$

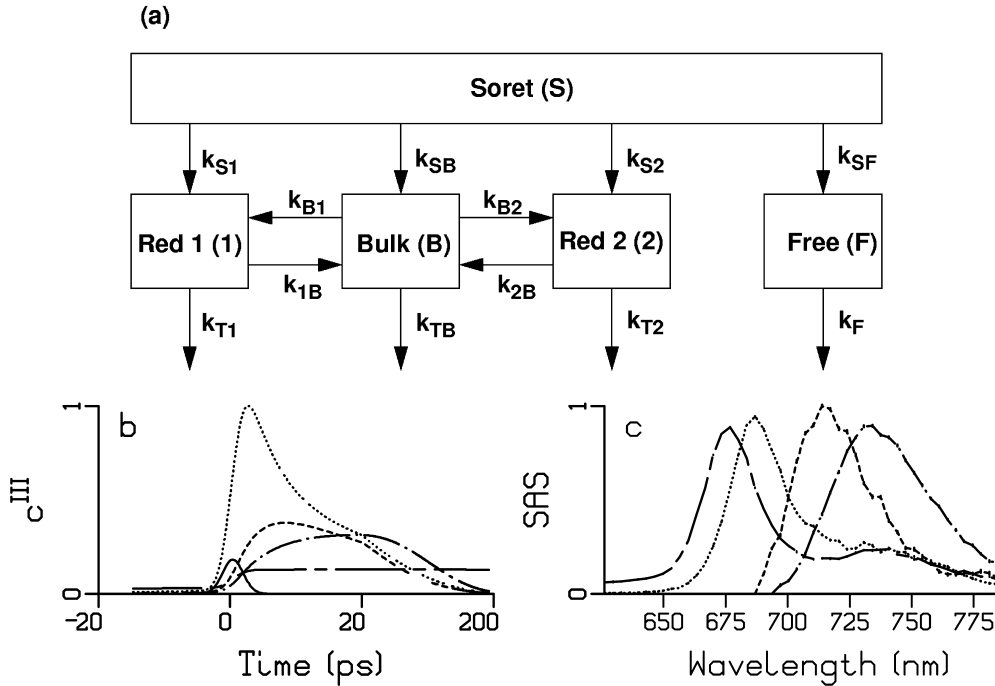


Fig. 5. (a) Kinetic scheme used for the target analysis of PS I data depicted in Fig. 1. After excitation in the Soret band four compartments are populated: bulk Chl *a* (B), two pools of red Chl *a* (1 and 2) and a small fraction of free Chl *a* (F). The first three compartments equilibrate, and excitations are trapped with different rates. (b) Concentration profiles c_l^{III} , note that the time axis is linear from -20 to +20 ps relative to the maximum of the IRF, and logarithmic thereafter. (c) Species Associated Spectra (SAS). Key in (b) and (c): bulk Chl *a* (dotted), red Chl *a* 1 (dashed), red Chl *a* 2 (dot dashed), free Chl *a* (chain dashed).